Scientific Researches in
Theoretical and Applied Physics
Vol. 2, Issue. 2, Fall 2024

Research Paper

# Sensing properties of various gas molecules on the Fe-doped upon vacancy-defected armchair antimonene nanoribbon

**Jamal Barvestani *[1], Sharareh Hasanpour Kashani [2], Bahar Meshginqalam [3]**



DOI: 10.22034/strap.2024.18575

Refference to this article: Barvestani, J; Hasanpour Kashani, S; Meshginqalam, B; (2024). Sensing properties of various gas molecules on the Fe-doped upon vacancy-defected armchair antimonene nanoribbon. *Scientific Researches in Theoretical and Applied Physics*, 2 (2): 19-34

**Keywords**

**Armchair antimonene nanoribbons; Vacancy defects; Gas molecules; Magnetic moment; Spin filter efficiency.**

**Received: 2024/06/10**

**Accepted: 2024/10/01**

**Available: 2025/07/08**

**A B S T R A C T**

The sensing properties of single vacancy defected and Fe atom doped armchair antimonene nanoribbons for $NO_2$, NO, $N_2$, $CO_2$, CO, $O_2$, $NH_3$, and $SO_2$ gases have been systematically studied using the first-principles calculations based on the density functional theory. The nanoribbon is doped with a magnetic Fe element after creating a single vacancy defect, and then the sensing properties of various molecules are examined. The results indicate that gas molecules are physisorbed on pure antimonene nanoribbon with low adsorption energy. However, all the gas molecules (except $N_2$) are chemisorption on Fe-doped upon single vacancy defected antimonene nanoribbons. The Adsorption behaviors of these gases have been analyzed in terms of band structure, the density of states, adsorption energy, magnetic moments, and I-V characteristics. We showed that the introducing single vacancy defects and doping of Fe atom improve the adsorption process. The NO molecule has strong adsorption and creates more stability on both bare and Fe-doped ASbNRs than the other gases, but the adsorption of $SO_2$ leads to the demagnetization of the system. Splitting of up and down spin currents occurs in the $CO_2$, $O_2$, CO, and $NH_3$ cases, which leads to high values of spin filter efficiency. Therefore, these results are helpful in the efficiency of antimonene-based gas sensors with high detection properties.

* **Corresponding Author: Jamal Barvestani**
**E-mail:** barvestani@tabrizu.ac.ir

1. Faculty of Physics, University of Tabriz.
2. Faculty of Physics, University of Tabriz.
3. Faculty of Physics, University of Tabriz.

مقاله پژوهشی

# خواص حسگری مولکولهای گازی متنوع در نانونوار آنتیمونن دسته‌صندلی آلاییده با آهن بر روی نقص تهی‌جا

جمال بروستانی[1]*، شراره حسن‌پور کاشانی[2]، بهار مشگین قلم[3]



**ارجاع به این مقاله:** بروستانی، جمال ؛ حسن‌پور کاشانی ، شراره ؛ مشگین قلم ، بهار (1403). خواص حسگری مولکولهای گازی متنوع در نانونوار آنتیمونن دسته‌صندلی آلاییده با آهن بر روی نقص تهی‌جا . *پژوهش‌های علمی در فیزیک نظری و کاربردی، 2(2) 34-19.*

DOI: 10.22034/strap.2024.18575

**چکیده**

خواص حسگری نانونوارهای آنتیمونن دسته‌صندلی دارای نقص تهی‌جا و آلاییده با اتم آهن برای گازهای $NO_2$، NO، $N_2$، $CO_2$، CO، $O_2$، $NH_3$ و $SO_2$ با استفاده از محاسبات ابتدا به ساکن بر اساس تئوری تابعی چگالی مورد مطالعه قرار گرفته‌اند. نانونوار پس از ایجاد یک نقص تهی‌جا ، با عنصر آهن مغناطیسی آلایش می‌یابد و سپس خواص حسگری مولکول های مختلف مورد بررسی قرار می گیرد. نتایج نشان می‌دهد که مولکول‌های گاز روی نانونوار آنتیمونن خالص با انرژی جذب پایین جذب فیزیکی می‌شوند. با این حال، همه مولکول‌های گاز (به جز $N_2$) به نانونوارهای آنتیمونن دارای نقص تهی‌جای آلاییده با آهن، جذب شیمیایی می‌شوند. رفتارهای جذب این گازها از نظر ساختار نواری، چگالی حالت‌ها، انرژی جذب، گشتاورهای مغناطیسی و ویژگی‌های I-V مورد تجزیه و تحلیل قرار گرفته‌اند. ما نشان داده‌ایم که معرفی نقص‌های تهی‌جا و آلایش اتم آهن فرآیند جذب را بهبود می‌بخشد. مولکول NO دارای جذب قوی است و پایداری بیشتری در هر دو ASbNR تهی‌جا و آاییده با آهن نسبت به سایر گازها ایجاد می کند، اما جذب $SO_2$ منجر به مغناطیس زدایی سیستم می شود. تفکیک جریان های اسپین بالا و پایین در موارد $CO_2$، $O_2$، CO و NH3 رخ می دهد که منجر به مقادیر بالایی از بازدهی فیلتر اسپین می شود. بنابراین، این نتایج در کارایی حسگرهای گاز مبتنی بر آنتی‌مونن با خواص تشخیص بالا مفید است.

**کلیدواژه‌ها**

**Armchair antimonene nanoribbons; Vacancy defects; Gas molecules; Magnetic moment; Spin filter efficiency.**

**دریافت شده: 1403/03/21**

**پذیرفته شده: 1403/07/10**

**منتشر شده: 1404/04/17**

* نویسنده مسئول: جمال بروستانی

رایانامه: barvestani@tabrizu.ac.ir

1- استاد، دانشکده فیزیک، دانشگاه تبریز.

2- دانشکده فیزیک، دانشگاه تبریز.

3- دانشکده فیزیک، دانشگاه تبریز.

## I. INTRODUCTION

Air pollution and diffusion of industrial wastewater are one of the basic environmental and sanitary problems of the world today [1]. The report of the World Health Organization shows that millions of people die since half of the world does not have access to clean air. Therefore, it is essential to recognition and detects toxic gases and thus reduces these gases in the environment. Today, the concentration of CO harmful gas has increased dramatically in the air. Therefore, huge research has been done for sensing different gases in all kinds of structures of different sizes, even bulky ones [2]. One of the features that make two-dimensional (2D) materials suitable for gas sensing, is the high surface-to-volume ratio. Some two-dimensional materials such as silicene, germanene, arsenene, and $MoS_2$ have an adsorption behavior similar to graphene due to their wonderful structure, and this feature has attracted a lot of attention. Therefore, 2D materials as anticipated candidates for detecting toxic gases have been investigated in the last few decades. Graphene is the first 2D material that was used to detect toxic gases NO, CO, $NO_2$, $NH_3$, etc. [3, 4]. Improvement of the magnetic and electronic properties of 2D materials for their application in gas sensing, rechargeable batteries, and spintronic is one of the most important issues that have been studied in the last few decades by using atom adsorption, doping, and heterostructure methods [5, 6]. In one of the studies, after doping, graphene was recognized as an effective detector of NO and $NO_2$ gases [7]. Mei et al. investigated the effect of doping $Ag_3$ on $WSe_2$ sensing. They studied the adsorption of three gases of $NH_3$, $NO_3$, and $Cl_2$ on pure $WSe_2$ and doped $WSe_2$ substrates. The results showed that the adsorption performance of these three gases on the substrate with $Ag_3$ is higher than its pure one [8]. Another study has been done on the adsorption of $H_2CO$ molecules on pure graphene and doped with Ti and V atoms, by Chen et al [9]. The results of this study are that Ti and V atoms increase the interaction between $H_2CO$ molecule and graphene. The desired molecule is chemically adsorbed on Ti and V atoms, with the band structure changing after the adsorption of the molecule [10]. Also, the results of Zhou et al.'s investigations on the detection of CO, $NO_2$, $H_2O$, and $NH_3$ gases on pure $MoS_2$ monolayer and doped with V, Nb, and Ta metals, shows that the doping of the mentioned metals causes the sensing and

adsorption properties of the desired gases are increased [11]. In another investigation, the sensing of $NO_2$ and $NH_3$ gases on the single layer of pure $MoS_2$ and doped with Al, Si, and P atoms has been studied. Doped MoS2 with Si and P atoms create a stable covalent bond between Si-Mo and P-Mo and behave as a semiconductor. Doped atoms increase the combination of orbitals between gases and $MoS_2$ monolayer so improve the electrons transfer. The adsorption of these gases also changes the magnetic moment of the doped structure. As a result, the doped $MoS_2$ monolayer shows better adsorption properties than the pure one [12]. However, the efficiency of these materials is limited due to some shortcomings. For example, graphene has a zero-band gap, and H-BN has a very wide band gap. In transition metal dichalcogenides, electron mobility is very low, and phosphorene has poor chemical stability. Therefore, it is necessary to discover other 2D materials with superior properties, including suitable band gap and more stability. Antimonene, a monolayer of Sb atoms, has different phases with various structures [13], which was first studied theoretically in 2015 [10]. Zhang et al. prove that among different phases, beta antimonene has the lowest configuration energy and therefore shows more stability [14, 15]. Antimonene was manufactured through mechanical and liquid phase exfoliation methods. In addition, by cutting antimonene in a specific direction, nanoribbons present an edge-dependent band structure and notable deformation potential [16, 17, 18, 19, 20]. To study the sensing properties of antimonene, the effects of CO and NO gas molecules on the electronic and transport properties of antimonene nanoribbons (SbNRs) have been studied by Srivastava et al. [18]. Their results show that the sensing capability of SbNRs progresses considerably when doped with silicon. In 2020, the adsorption capacity of $CO_2$ and $NH_3$ molecules on SbNRs has been studied [21]. Results indicate that the band structure of ZSbNRs shows less modification after adsorption, but the band structure of ASbNRs varies from semiconductor to metallic after adsorption. Tang et al. studied the adsorption effects of various toxic gas molecules in ZSbNRs [22]. Their results show that $NO_2$ gas molecules create chemical bonds with ZSbNRs, but $PH_3$ and $H_2S$ have fragile adsorption. Also, it is found that $SO_2$, $NH_3$ and NO have great adsorption energy and change current significantly after adsorption. Therefore, ZSbNRs are strongly gas-sensing sensors for $SO_2$, $NH_3$, and NO [22]. Chen et al. studied the adsorption of NO molecule on

the vacancy-defected and (Sc, Ti) doped antimonene in 2023 [23]. Due to the fact that in pure structure, the NO molecule has physical adsorption with low adsorption energy, hence applying defects and doping impurities causes' chemisorption, so the adsorption energy increases. There is another study in 2023 on the sensing properties of antimonene, which is investigated the sensing effects of different gases on the Fe-decorated monolayer antimonene [24].Their results indicate that chemisorption processes can be achieved for CO, COS, NO and $NO_2$, but $NH_3$ and $SO_3$ have physical adsorption. Furthermore, previous studies show that doping [25] and strain [26] improve the adsorption properties. To the best of our knowledge, there are very few reports on the adsorption of gas molecules in the structure of antimonene. On the other hand, studies on the modification of materials have been done solely on doping impurities or structural defects. In this work, we investigated the adsorption effect of eight gas molecules on the Fe-doped upon single vacancy-defected ASbNRs (Fe-SV-ASbNRs). The band structures, density of states and magnetic moments are calculated using density functional theory (DFT) and the results are compared extensively.

## II. COMPUTATIONAL METHODS

In this article, all the calculations are based on the density functional theory (DFT) which are implemented in Atomistix Tool Kit (ATK) simulation software [27]. We used Perdew, Burke and Ernzerhof (PBE) to estimate the exchange-correlation functional with spin generalized gradient approximation (SGGA) between the electrons [28]. The electron wave function was explained by the Fritz Haber Institute (FHI) pseudopotential and double zeta polarized (DZP) basis set. The density mesh cut-off is set to 150 Ry. The 1×1×21 k-point mesh is set for geometry optimization, and the 1×1×100 is sufficient for the magnetic calculations and the transport properties. For optimization calculations, the atom force and stress on each atom were set to 0.05 eV/Å and 0.005 eV/$Å^3$, respectively. By choosing the mentioned values for density mesh cut-off and K-point sampling, the convergency speed increased and the suitable results were obtained. We considered vacuum distance about 20 Å due to eliminating the interaction between nearby layers.

## III. RESULTS AND DISCUSSION

To study the adsorption properties of gas molecules ($NO_2$, NO, $N_2$, $CO_2$, CO, $O_2$, $NH_3$, and $SO_2$) on bare and Fe-doped SV-ASbNRs

substrate, we took a supercell of ASbNRs in beta phase with nine atoms in width as shown in Figure 1. All the investigated structures are optimized firstly, according to the mentioned parameters, and the bond length and buckling height are selected as 2.87 Å and 1.65 Å [29], respectively. First, the depicted atom with an arrow in panel a is removed and then a Fe atom is substituted at vacated position. The optimized structure of Fe-doped SV-ASbNR with $SO_2$ molecule, for example, is shown in Figure 1(c). As can be clearly observed from Figure 1, the gas molecule is placed on the top of the Fe atom and a single vacancy.

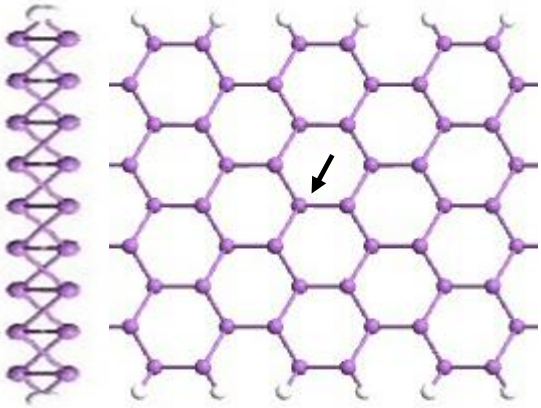

(a)

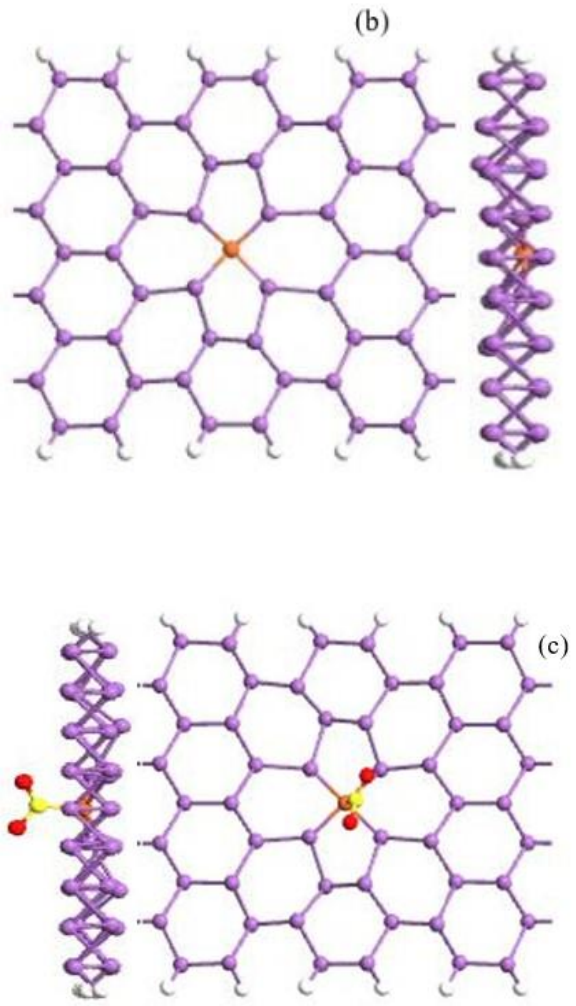


Figure **1**. Top and side views of the most stable structures of pure antimonene (a), Fe-doped SV-ASbNR (b), $SO_2$ adsorbed on Fe-doped SV-ASbNR (c). The Sb, H, Fe, S and O atoms are shown in purple, white, orange, yellow and red balls, respectively.

The band structure of pure ASbNR and Fe-doped SV-ASbNR substrates is plotted, in Figure 2. The bare ASbNR has a direct band gap with a band gap of 1.61 eV (without any splitting of spin-up and down bands), as shown in Figure 2. On the other hand, the

case of the Fe-SV-ASbNR indicates that the spin-up and down bands are split completely, which show a magnetic semiconductor property and also, many other defect bands are appear within the bandgap.

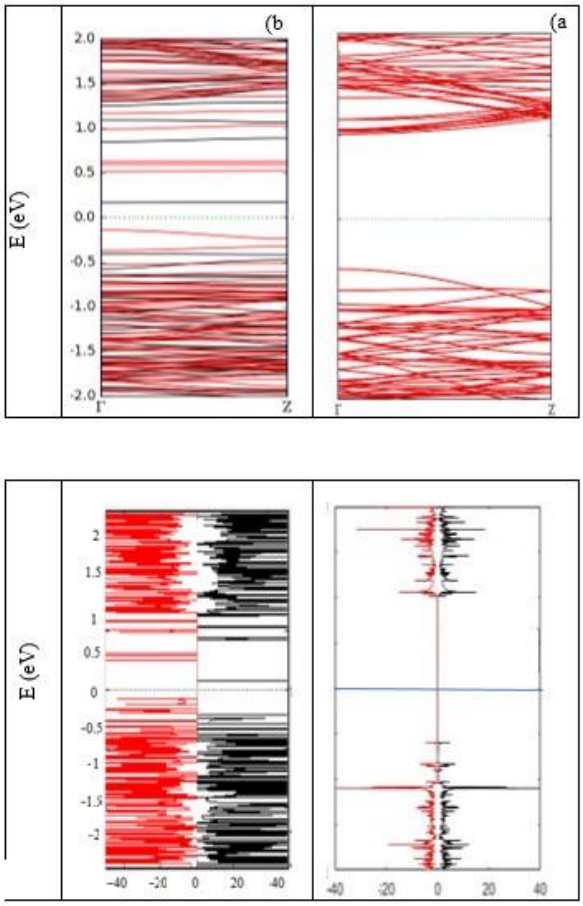


Figure **1.** Band structure for a) pure ASbNR b) Fe-doped SV-ASbNRs. Lower panel show the corresponding density of states.

The stability of the adsorption configuration of various gas molecules on the nanoribbons is estimated by calculating the adsorption energies, which are defined as $E_{ads} = E_{g+s} - E_g - E_s$ [30], where $E_{g+s}$, $E_g$, and $E_s$ represent the total energy of the gas molecule adsorption on a bare/defected antimonene in fully relaxed structure, a single gas molecule, and pristine/defected antimonene, respectively. The adsorption energy of eight different molecules on bare ASbNRs and Fe-doped SV-ASbNRs are summarized in Table 1.

Table **1.** The adsorption energy ($E_{ads}$) for all of the considered gas molecules ($NO_2$, NO, $N_2$, $CO_2$, CO, $O_2$, $NH_3$, and $SO_2$) in the bare ASbNRs and Fe-doped SV-ASbNRs.

| $E_{ads}$ (eV) | $NO_2$ | NO | $N_2$ | $CO_2$ | CO | $O_2$ | $NH_3$ | $SO_2$ |
|---|---|---|---|---|---|---|---|---|
| bare case | -0.54 | -0.86 | -0.25 | -0.28 | -0.14 | 0.085 | -0.36 | -0.72 |
| Fe-doped SV-ASiNR | -2.08 | -3.57 | -0.3 | -0.37 | -2.39 | -1.55 | -1.06 | -1.75 |

By comparing the adsorption energies of the pristine and defective substrates, it is concluded that the gas molecules have very weak adsorption in the bare case, hence the adsorption energies are low compared with a defective case. Thus, the Fe doping process helps considerably to strengthen the cohesion of these gases to defected nanoribbons. Among the gases, the NO molecule has a high adsorption energy compared to other molecules; therefore, it is more stable. After

optimization, the adsorption distance of $NO_2$, NO, $N_2$, $CO_2$, CO, $O_2$, $NH_3$, and $SO_2$ gases in the Fe-doped SV-ASbNR are 1.84, 1.60, 2.51, 2.01, 1.70, 1.89, 1.98, and 2Å, respectively. The bond length between gas molecules and Fe atom is reduced by about 1.3-0.12 Å compared to the adsorption distance in the pure structure. To realize the reason for the enhancement of adsorption energy and the prospect of the interaction between substrate and different gases, the band structures are shown in Figure 4. Red (black) curves denote down (up) spin bands in each case.

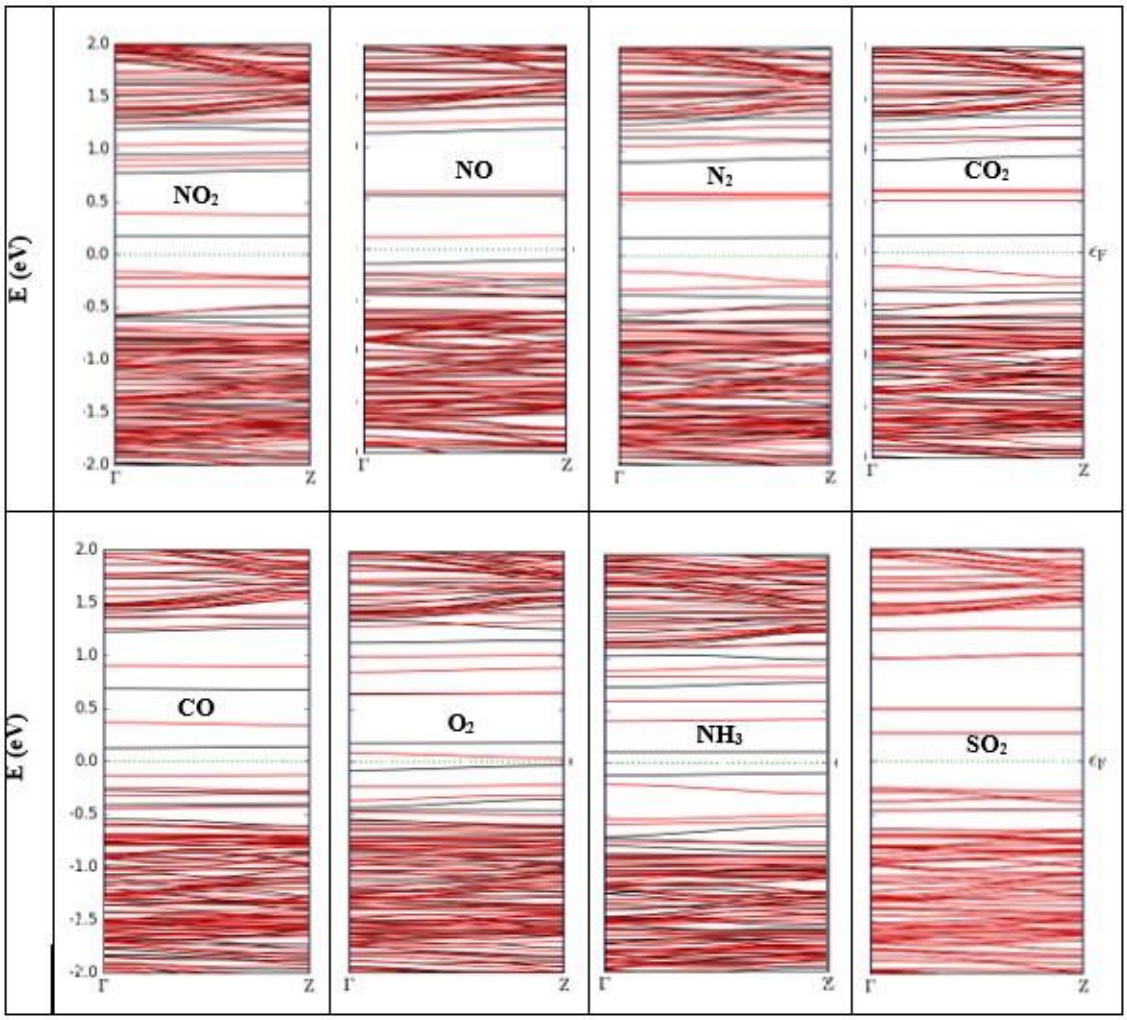


Figure **3.** Band structure of Fe-doped SV- ASbNR adsorbed with gas molecules ($NO_2$, NO, $N_2$, $CO_2$, CO, $O_2$, $NH_3$ and $SO_2$).

In the case of the pure substrate, among all the gases, we have had spin splitting only for the cases of the adsorption of NO and $NO_2$ gases (the corresponding band structures are not presented here). In the defective structure, before the molecules are adsorbed, spin splitting occurs in all cases. The nanoribbons are completely magnetized after applying the mentioned changes; so, the defective substrates are magnetic semiconductors. According to Figure 3, the adsorption of the different molecules maintains its magnetic behavior. However, only the $SO_2$ molecule demagnetizes the magnetized substrate and causes the degeneration of up and down spins. To understand the effect of the gases adsorption on the magnetic properties of bare and SV-ASbNR, we calculate the magnetic moments for all of the considered gas molecules and tabulated the results, in Table 2.

Table **2** The corresponding magnetic moments for all the considered gases in the bare and Fe-doped SV-ASbNRs.

| **Magnetic moment ($\mu_B$)** | **$NO_2$** | **NO** | **$N_2$** | **$CO_2$** | **CO** | **$O_2$** | **$NH_3$** | **$SO_2$** |
|---|---|---|---|---|---|---|---|---|
| The bare case | 1.013 | 1.00 | 0 | 0.004 | 0 | 0 | -0.005 | 0 |
| The Fe-doped-SV case | 1.004 | 0.985 | 1.998 | 2.003 | 0.036 | 1.793 | 1.999 | 0.005 |

The tabulated values of the magnetic moments are consistent with the result of the band structure of the corresponding gas. However, the magnetic moment of NO and $NO_2$ cases do not vary considerably via doping processes. For the other cases, the magnetic moments are modified, significantly.

Finally, to further investigate the sensing behavior of considered gases in the defective substrate, we have studied the transport properties via current-voltage simulation. Figure 4, shows the proposed transistor structure of antimonene-based sensor for eight gas molecules, schematically.

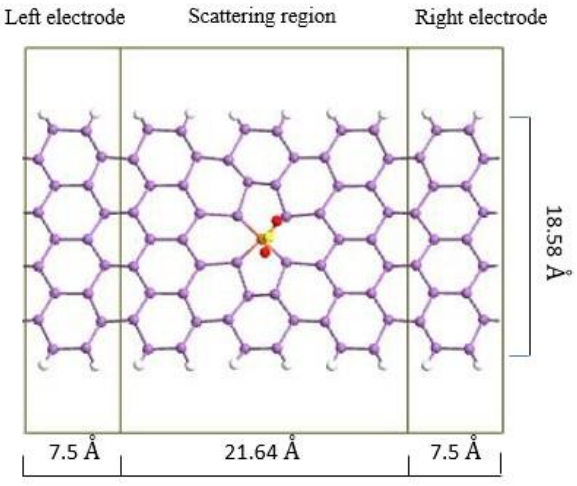


Figure **4.** The structure of defective ASbNR-based sensor for toxic gas molecule (simulated configurations)

Figure 5, shows the I-V characteristic for eight different gas molecules adsorbed on Fe-doped SV-ASbNRs. Black curves correspond to the spin currents of Fe-doped SV-ASbNRs in the presence of adsorbed gas molecules. For comparison purposes, red curves denote the currents without gas molecules, which are identical in all cases. The up (down) spin currents are represented by a solid (dashed) line.

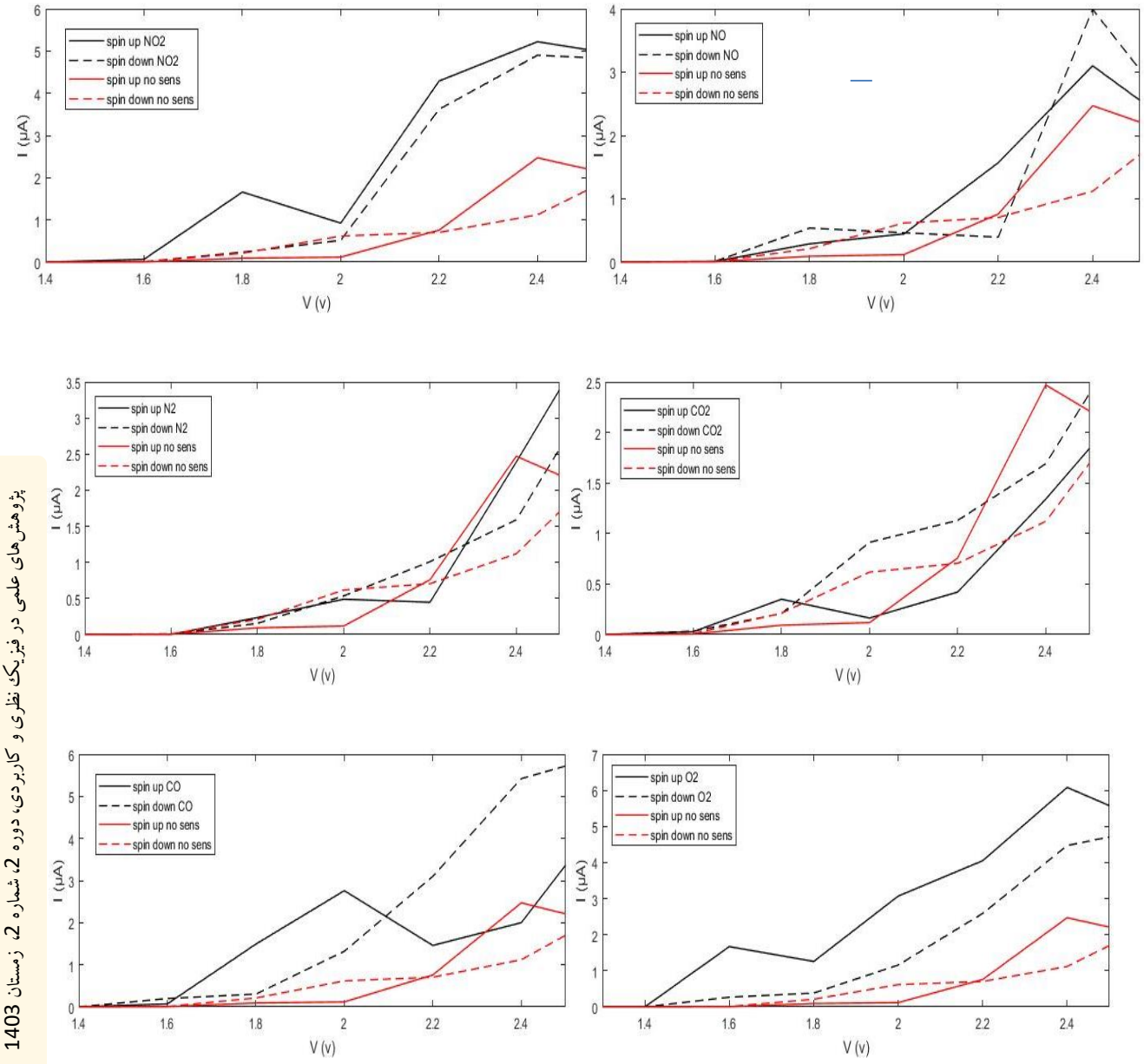

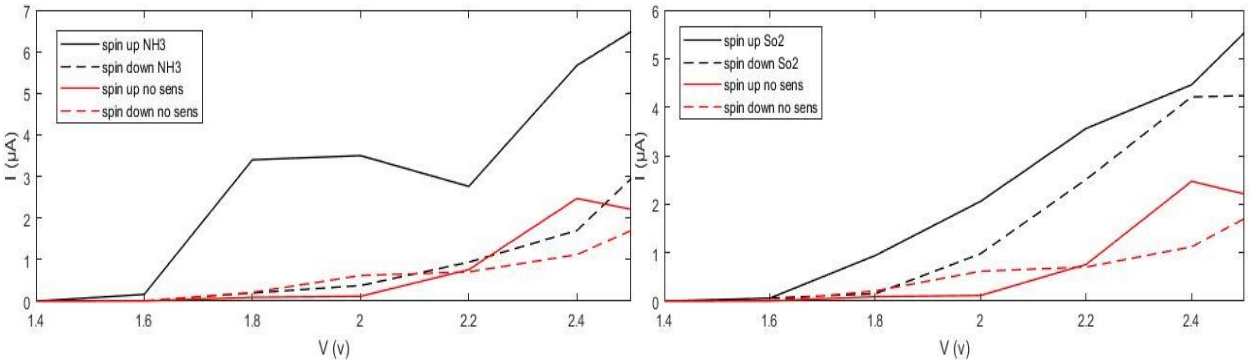


Figure **5.** The current – voltage curves for the adsorbed Fe doped SV-ASbNR transistor with $NO_2$, NO, $N_2$, $CO_2$, CO, $O_2$, $NH_3$ and $SO_2$ gases (black curves). Red curves display currents in the absence of gas molecules.

These figures show that the adsorption of $NO_2$, NO, $N_2$, $CO_2$, CO, $O_2$, $NH_3$, and $SO_3$ gases on the Fe-doped SV-ASbNR causes changes in up and down spin currents. The threshold voltage for all cases (except for $O_2$ case which is reduced to 1.4 V) is approximately 1.6 V and is consistent with the band gap value of the ASbNR structure. As we can see, the trends of currents are different for various molecules. In the case of $NO_2$, $O_2$, and $SO_2$ molecules, both up and down spin currents increase compared to the structure without molecules. Also, in CO, $NH_3$, $N_2$, and NO gases, the up and down spin currents behave differently, so that the values of the up-spin currents in NO are more than non-adsorbing structure, but in $N_2$ and CO molecules, the spin currents are lower than the non-adsorbing structures. In the case of the $NH_3$ molecule, the up-spin current is more than those of the structure without the molecule, but the down-spin currents are equal up to 1.2 V and after that, the down-spin current of the adsorbing structure increases. The spin currents of the $CO_2$ molecule also behave in such a way that the down-spin current of the adsorbing structure is more and the up-spin current (after 2 V) is less than the non-adsorbing structure.

The spin filter efficiency (SFE) is one of the main characteristic features of spintronic devices, which is defined as $SFE = \left|\frac{I_{up}-I_{down}}{I_{up}+I_{down}}\right| \times 100$, to show better the differences between up and down currents [31]. $I_{up}$ ($I_{down}$) demonstrates the up (down) spin current. For a more accurate and better comparison of the SFE results, the curves of different gases are given in Figure 6.

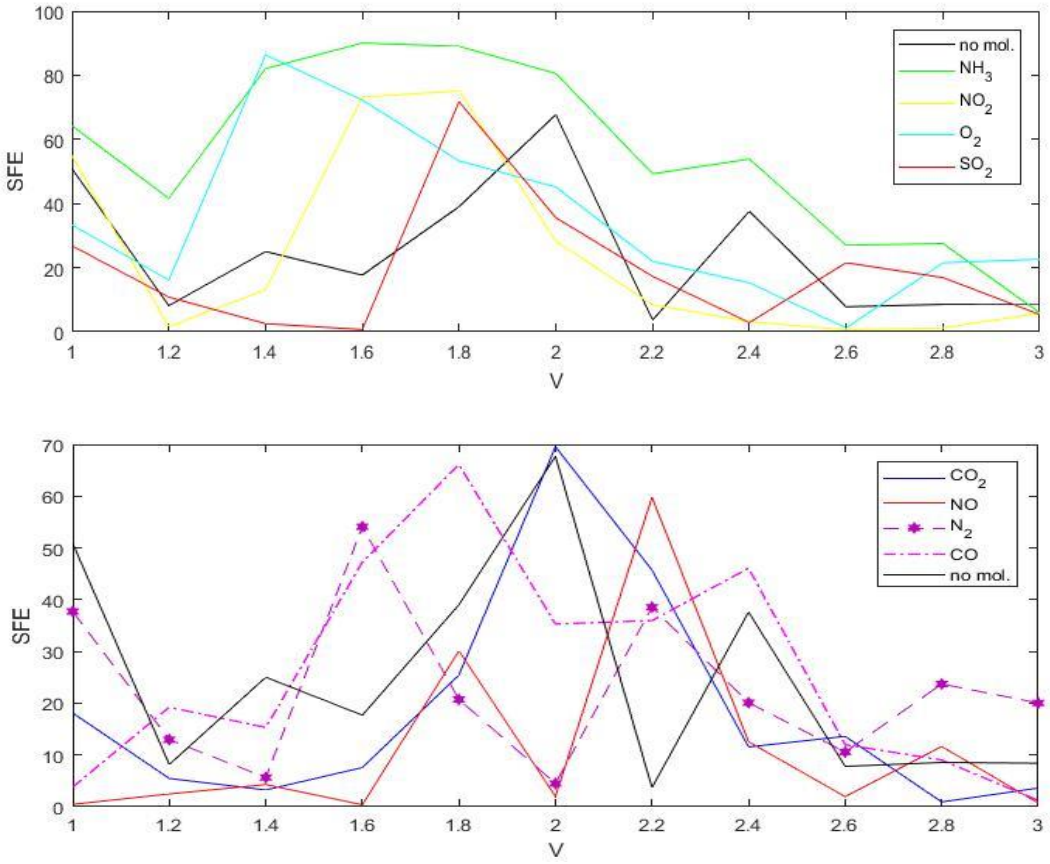


Figure **6.** The spin filter efficiency of Fe-doped SV-ASbNR adsorbed with eight different gases

According to Figure 6(a), the highest value of SFE corresponds to $NH_3$ gas. Also, as voltage increases, the SFE value for all three gases, $NH_3$, $NO_2$ and $O_2$, has a decreasing trend, but the structure without the gas molecules does not behave uniformly. In Figure 6(b), we see the indistinctive behavior of gas molecules, so that except for $CO_2$ and $SO_2$ molecules, the rest of the gases have two peaks in the applied voltage range. As expected from the current-voltage characteristic, the SFE of $CO_2$ gas increased to 2 V and then decreased due to the closeness of the up and down spin current values.

## IV. CONCLUSION

In summary, we have studied the adsorption effects of $NO_2$, NO, $N_2$, $CO_2$, CO, $O_2$, $NH_3$, and $SO_2$ gases on bare ASbNR and Fe-doped SV-ASbNRs using DFT calculations. Due to the physical adsorption of gas molecules on the pure substrate, it is found that the pure structure is insensitive to gas molecules. Introducing a single vacancy defect and Fe doping increases the sensing ability of

antimonene structures, so gas molecules are chemisorption on Fe-doped single vacancy defected antimonene nanoribbons. Adsorption energy analyses show that adsorbing NO gas on both structures (bare and Fe-doped SV-ASbNRs) has stronger adsorption than the other mentioned gases. In addition, the band structure results indicate that the $SO_2$ molecule demagnetizes the magnetic substrate, so it reduces the magnetic moment to zero. The magnetic moment values of $N_2$, $CO_2$, $O_2$, and $NH_3$ gases adsorption in defective substrate have increased compared to the pure one. Among the desired gases, $NO_2$, NO, CO, $SO_2$, $O_2$, and $NH_3$ gas have higher values of spin current than those of the structure without molecules. Splitting of up and down spin currents occurs in the $CO_2$, $O_2$, CO, and $NH_3$ cases, which leads to high values of spin filter efficiency. Therefore, the results demonstrate that the Fe-doped SV-ASbNR properties may provide a new path for fabricating desirable gas sensors.

## REFERENCES


[1] V. Ramanathan and Y. Feng, "Air pollution, greenhouse gases and climate change: Global and regional perspectives," *Atmospheric Environment,* vol. 43, p. 37, 2009.

[2] K. Patel, B. Roondhe, S. D. Dabhi and P. K. Jha, "A new flatland buddy as toxic gas scavenger: A first principles study," *Journal of Hazardous Materials,* vol. 351, p. 337, 2018.

[3] Y. Zeng, S. Lin, D. Gu and X. Li, "Two-dimensional nanomaterials for gas sensing applications: the role of theoretical calculations," *Nanomaterials,* vol. 8, p. 85, 2018.

[4] O. Leenaerts, B. Partoens and F. Peeters, "Adsorption of $H_2O$, $NH_3$, CO, $NO_2$, and NO on graphene: a first-principles study," *Phys. Rev. B,* vol. 77, p. 125416, 2008.

[5] B. Meshginqalam and J. Barvestani, "Doped Arsenene Nanoribbon as a Promising Candidate for Sensing Toxic Gas Molecules: Theoretical Approach," *IEEE SENSORS JOURNAL,* vol. 20, no. 11, p. 5984, 2020.

[6] B. Meshginqalam and J. Barvestani, "Highly sensitive toxic gas molecule sensor based on defect-induced silicene," *JOURNAL OF MATERIALS SCIENCE-MATERIALS IN ELECTRONICS,* vol. 30, p. 18637, 2019.

[7] J. Zhang, X. Liu, G. Neri and N. Pinna, "Nanostructured materials for room-temperature gas sensors," *Adv. Mater.,* vol. 28, p. 795, 2016.

[8] H. Mi, Q. Zhou and W. Zeng, "A density functional theory study of the adsorption of $Cl_2$, $NH_3$, and $NO_2$ on $Ag_3$-doped $WSe_2$ monolayers," *Appl. Surf. Sci.* , vol. 563, p. 150329, 2021.

[9] X. Chen, L. Xu, L. L. Liu, L. S. Zhao, C. P. Chen, Y. Zhang and X. C. Wang, "Adsorption of formaldehyde molecule on the pristine and transition metal doped graphene: first-principles study," *Appl. Surf. Sci.*, vol. 396, p. 1020, 2017.

[10] J. Zhou, H. Zhang, Y. Tong, L. Zhao, Y. Zhang, Y. Qiu and X. Lin, "First-principles investigations of metal (V, Nb, Ta)-doped monolayer $MoS_2$: Structural stability, electronic properties and adsorption of gas molecules," *Appl. Surf. Sci.*, vol. 419, p. 522, 2017 .

[11] H. Luo, Y. Cao, J. Zhou, J. Feng, J. Cao and H. Guo, "Adsorption of $NO_2$, $NH_3$ on monolayer $MoS_2$ doped with Al, Si, and P: a first-principles study," *Chem. Phys. Lett.*, vol. 643, p. 27, 2016.

[12] C. Gibaja, D. Rodriguez, P. Ares, J. Gomez and M. Varela, "Few-layer antimonene by liquid-phase exfoliation," *Angew. Chem. Int. Ed.*, vol. 55, p. 14345, 2016.

[13] S. Zhan, M. Xie, F. Li, Z. Yan, Y. Li, E. Kan, W. Liu, Z. Chen and H. Zeng, "Semiconducting Group 15 Monolayers: A Broad Range of Band Gaps and High Carrier Mobilities," *Angew. Chem.*, vol. 128, p. 1698, 2016.

[14] P. Ares, F. Aguilar-Galindo, D. Rodriguez-San-Miguel, D. A. Aldave, S. DiazTendero, M. Alcami, F. Martin, J. Gomez-Herrero and F. Zamora, "Mechanical isolation of highly stable antimonene under ambient conditions," *Adv. Mater.*, vol. 28, p. 6332, 2016.

[15] C. Gibaja, D. Rodriguez-San-Miguel, P. Ares, J. Gómez-Herrero, M. Varela, R. Gillen, J. Maultzsch, F. Hauke, A. Hirsch, G. Abellán and F. Zamora, "Few-layer antimonene by liquid-phase exfoliation," *Angew. Chem. Int. Ed.*, vol. 55, p. 14345, 2016.

[16] O. Ü. Aktürk, V. O. Özçelik and S. Ciraci, "Single-layer crystalline phases of antimony: Antimonenes," *Phys. Rev. B*, vol. 91, p. 235446, 2015.

[17] Y. Wang and Y. Ding, "Electronic Structure and Carrier Mobilities of Arsenene and Antimonene Nanoribbons: A First-Principle Study," *Nanoscale Res. Lett.*, vol. 10, p. 254, 2015.

[18] V. Nagarajan and R. Chandiramouli, "Sensing studies of DDT and Toxaphene molecules using chemi-resistive β-antimonene nanotubes based on first-principles insights," *Chemical Physics Letters*, vol. 757, p. 137895, 2020.

[19] Y. Song, X. Wang and W. Mi, "Spin splitting and electric field modulated electron-hole pockets in antimonene nanoribbons," *NPJ Quantum Mater*, vol. 2, p. 15, 2017.

[20] A. C. R. Souzal, M. J. S. Matos and M. S. C. Mazzoni, "A. C. R. Souzal, M. J. S. Matos and M. S. C. Mazzoni, "Oxidation-driven formation of precisely ordered antimonene nanoribbons," *J. Phys.: Condens. Matter*, vol. 32, p. 165302, 2019.

[21] P. Sirvastava, V. S. Abhishek and N. K. Jaiswal, "First-principles investigation of $CO_2$ and $NH_3$ adsorption on antimonene nanoribbons," *Materials Today: Proceedings*, vol. 28, p. 65, 2020.

[22] X. Tang and H. Zou, "Gas-sensitive Properties of Adsorping Toxic Gases on Antimonene Nanoribbons," *International*

material," *Journal of Materials Chemistry A*, vol. 496, p. 1099, 2019.

[27] Atomistix ToolKit, vresion 2016.04, Quantum Wise A/S. www.quantumwise.com.

[28] J. Perdew, K. Burke and M. Ernzerhof, "Generalized gradient Approximation made simple," *Physical review letters*, vol. 77, p. 3865, 1996.

[29] S. B. Touski and M. P. López-Sancho, "Effects of vertical electric field and charged impurities on the spin-polarized transport of β-antimonene armchair nanoribbons," *Physical Review B*, vol. 103, p. 115433, 2021.

[30] R. Deji, A. Verma, N. Kaur, B. C. Choudhary and R. K. Sharma, "Density functional theory study of carbon monoxide adsorption on transition metal doped armchair graphene nanoribbon," *Materials Today: Proceedings*, vol. 54, p. 771, 2022.

*Symposium on Next Generation Electronics*, vol. 56, p. 1, 2021.

[23] G.-X. Chen, R.-Y. Du, D.-D. Wan, Z. Chen, S. Liu and J.-M. Zhang, "Adsorption of NO gas molecule on the vacancy defected and transition metal doped antimonene: A first-principles study," *Vacuum*, vol. 207, p. 111654, 2023.

[24] M. I. Khan, M. Hassan, A. Majid, M. Shakil and M. Rafique, "DFT perspective of gas sensing properties of Fe-decorated monolayer antimonene," *Applied Surface Science*, vol. 616, p. 156520, 2023.

[25] F. Safari, M. Moradinasab, M. Fathipour and H. Kosina, "Adsorption of the $NH_3$, NO, $NO_2$, $CO_2$, and CO gas molecules on blue phosphorene: a first-principles study," *Applied Surface Science*, vol. 464, p. 153, 2019.

[26] C. Jin, X. Tang, X. Tan, S. C. Smith, Y. Dai and d. L. Kou, "A Janus MoSSe monolayer: a superior and strain sensitive gas sensing

[31] D. Zhang, M. Long, X. Zhang, F. Ouyang, M. Li and H. Xu, "Designing of spin-filtering devices in zigzag graphene nanoribbons heterojunctions by asymmetric hydrogenation and B-N doping," *J. Appl. Phys.*, vol. 117, p. 014311, 2015.